The Plant Cell, Vol. 16, 1047–1059, April 2004, www.plantcell.org

Enod40, a Short Open Reading Frame–Containing mRNA, Induces Cytoplasmic Localization of a Nuclear RNA Binding Protein in *Medicago truncatula*

Anna Campalans, Adam Kondorosi, and Martin Crespi[1]

Institut des Sciences du Végétal, Centre National de la Recherche Scientifique, 91198 Gif sur Yvette, France

In eukaryotes, diverse mRNAs containing only short open reading frames (sORF-mRNAs) are induced at specific stages of development. Their mechanisms of action may involve the RNA itself and/or sORF-encoded oligopeptides. *Enod40* genes code for highly structured plant sORF-mRNAs involved in root nodule organogenesis. A novel RNA binding protein interacting with the *enod40* RNA, MtRBP1 (for *Medicago truncatula* RNA Binding Protein 1), was identified using a yeast three-hybrid screening. Immunolocalization studies and use of a MtRBP1-DsRed2 fluorescent protein fusion showed that MtRBP1 localized to nuclear speckles in plant cells but was exported into the cytoplasm during nodule development in *enod40*-expressing cells. Direct involvement of the *enod40* RNA in MtRBP1 relocalization into cytoplasmic granules was shown using a transient expression assay. Using a (green fluorescent protein)/MS2 bacteriophage system to tag the *enod40* RNA, we detected in vivo colocalization of the *enod40* RNA and MtRBP1 in these granules. This in vivo approach to monitor RNA–protein interactions allowed us to demonstrate that cytoplasmic relocalization of nuclear proteins is an RNA-mediated cellular function of a sORF-mRNA.

INTRODUCTION

Short open reading frame mRNAs (sORF-mRNAs) are unusual mRNAs containing only sORFs (<100 amino acids) that accumulate in the cytoplasm (in many cases abundantly) where they may be translated into oligopeptides (MacIntosh et al., 2001). Their mechanisms of action may involve the RNA itself and/or sORF-encoded oligopeptides. sORF-encoded oligopeptides may act as signals in development (Lindsey et al., 2002), as has been suggested for the POLARIS oligopeptide (Casson et al., 2002). In certain sORF-mRNAs, conservation at nucleotide level but not at amino acid level suggests that the RNA can play an important role in the function of the gene, and they are referred to as noncoding RNAs (Furini et al., 1997; Erdmann et al., 2001; MacIntosh et al., 2001). Noncoding RNAs have been shown to participate in diverse processes, such as organization of the embryo cytoplasm, mRNA translation or stability, and protein secretion or silencing (Kelley and Kuroda, 2000; Kiss, 2002; Joyce, 2002). Moreover, translation of sORFs present in the sORF-mRNAs may occur even though the main function of the gene lies in the RNA product, as shown for a 5–amino acid sORF encoded in the 23S rRNA in *Escherichia coli* (Tenson et al., 1996), or the immunological detection of a putative protein encoded by the H19 gene (Leibovitch et al., 1991; Leighton et al., 1995). Indeed, several RNAs originally described as noncoding were shown to code for small peptides and vice versa (Eddy, 2002).

sORF-mRNA genes constitute a thus far unexplored component of the transcriptome; because of the small size of the encoded sORFs, they have eluded bioinformatical searches. However, there is accumulating evidence that they constitute an emerging class of genes. For example, in yeast (*Saccharomyces cerevisiae*), 18 previously unannotated sORF-mRNA transcripts were identified by biochemical means (Olivas et al., 1997), and five unusual noncoding transcripts have been identified to be specifically induced during meiosis (Watanabe et al., 2001). A bioinformatic analysis of the Arabidopsis (*Arabidopsis thaliana*) genome has identified 40 new putative noncoding RNAs or peptide-coding RNAs (MacIntosh et al., 2001). However, the molecular mechanisms involving sORF-mRNAs or their encoded oligopeptides are largely unknown.

mRNAs associate with RNA binding proteins to form ribonucleoprotein particles (RNPs) involved in processing, nucleocytoplasmic transport, localization, translation, and/or stability of mRNAs. In these processes, the protein components of the RNPs (RNA binding proteins [RBPs]) are thought to play crucial roles (Dreyfuss et al., 2002; Joyce, 2002). The RNA molecules presumably forming part of larger ribonucleoprotein complexes may play novel intracellular roles as shown for the intron-encoded small nucleolar RNAs (Kiss, 2002), the microRNAs (Hannon, 2002), or the BC1 transcript in mammals (Zalfa et al., 2003). The RNA molecule seems to determine the functional specificity of the complex, and analysis of mRNA–protein interactions may reveal novel RNA functions in these cellular complexes. The sORF-mRNAs may constitute examples that have retained specific mRNA functions. A function for an mRNA

[1] To whom correspondence should be addressed. E-mail crespi@isv.cnrs-gif.fr; fax 33-1-69823695.
The author responsible for distribution of materials integral to the findings presented in this article in accordance with the policy described in the Instructions for Authors (www.plantcell.org) is: Martin Crespi (crespi@isv.cnrs-gif.fr).
Article, publication date, and citation information can be found at www.plantcell.org/cgi/doi/10.1105/tpc.019406.

derived from a pseudogene (also a sORF-mRNA) in transcript stability has been demonstrated recently, further reinforcing the idea that both the mRNA and the encoded proteins may be functional products of a gene (Hirotsune et al., 2003).

Leguminous plants have the ability to enter into symbiosis with N_2-fixing bacteria (rhizobia) to form a new organ, the root nodule. Development of this symbiotic organ depends on the coordinated expression of plant and bacterial genes (Crespi and Galvez, 2000). The early nodulin gene *enod40* is rapidly induced by rhizobia in the root pericycle and in the dividing cortical cells of the nodule primordium (Compaan et al., 2001) as well as in other nonsymbiotic organs (Crespi and Galvez, 2000). A remarkable feature of *enod40* genes is that they contain only sORFs. Transgenic *Medicago truncatula* plants overexpressing *enod40* exhibited accelerated nodulation, whereas plants with reduced amounts of *enod40* transcripts formed only a few and modified nodule-like structures (Charon et al., 1999). The *enod40* genes are highly conserved in various leguminous species and also have been found in *Nicotiana tabacum* (tobacco) and rice (*Oryza sativa*) (Kouchi et al., 1999). Two highly conserved regions have been distinguished: Box I in the 5′ end, containing a conserved sORF, and Box II in the central part of the gene. Microtargeting of the *enod40* cDNA into *M. sativa* (alfalfa) roots induced division of cortical cells, and translation of two sORFs spanning Box I and Box II was required for this biological activity (Sousa et al., 2001). Indeed, sORF-encoded oligopeptides in the *enod40* RNA seem to be translated, although no direct proof has been obtained for their production in vivo (van de Sande et al., 1996; Compaan et al., 2001; Sousa et al., 2001; Rohrig et al., 2002). Recently, two *enod40*-encoded oligopeptides from *Glycine max* (soybean) have been shown to bind sucrose synthase in vitro (Rohrig et al., 2001); however, the lack of conservation of one of these peptides in other legume species makes its involvement unlikely in a general mechanism of *enod40* action. The *enod40* RNA is highly structured (Crespi et al., 1994) and not associated to polysomes (Asad et al., 1994). Secondary RNA structures seem to be required for the elicitation of the cell-specific growth response in *M. sativa* roots (Sousa et al., 2001). The secondary structure of the *G. max enod40* RNA has been determined recently, which has allowed the identification of five conserved domains in the *enod40* RNAs of numerous leguminous species (Girard et al., 2003). In particular, several motifs, such as U-containing stem-loops and bulges, have been found to be conserved. An implication of these stem-loops in protein recognition has been suggested by the authors (Girard et al., 2003). Hence, it appears that the RNA plays a crucial role in the molecular mechanism involved in the action of *enod40*.

To investigate cellular functions of the *enod40* RNA, we sought potential protein partners of the transcripts using the yeast three-hybrid system (Sengupta et al., 1996) to screen a *M. truncatula* cDNA library (Gyorgyey et al., 2000). One of the isolated clones encodes a novel RBP, MtRBP1 (for *M. truncatula* RNA Binding Protein 1), containing a nuclear localization signal (NLS) and a C-terminal region carrying an RNA recognition motif (RRM) and rich in Ser and Gly. Immunolocalization experiments as well as translational fusions to the DsRed2 fluorescent protein revealed the localization of MtRBP1 in nuclear speckles and its relocalization in the cytoplasm of *enod40*-expressing cells of the nodule. By cointroduction of *enod40* and MtRBP1 in *Allium cepa* (onion) cells and using a novel method to monitor RNA–protein interactions in vivo, we showed that this activity depended on the *enod40* RNA. Our results demonstrate that relocalization of a nuclear RBP is a novel function of the *enod40* sORF-mRNA.

RESULTS

Three-Hybrid Screening Revealed a Novel Protein, MtRBP1, Interacting with the *enod40* RNA

The yeast three-hybrid system is a powerful approach to detect RNA–protein interactions in living cells (Sengupta et al., 1996). The method consists of expressing three different hybrid molecules in yeast cells. A first hybrid protein consists of the MS2 coat protein fused to the GAL4 binding domain, a hybrid RNA consisting of the RNA of interest containing two tandem MS2 binding sites and a second hybrid protein in which the protein of interest (or a cDNA library to look for unknown partners) is fused to the GAL4 activation domain. The formation of an RNA protein complex approximates the GAL4 activation and binding domains resulting in transcriptional activation of two reporter genes (*HIS3* and *lacZ*). In our case, plasmids expressing either MS2-*enod40* or MS2-stem RNAs (the latter spanning a predicted stem derived from *enod40* RNA, indicated with an asterisk in Figure 1C) were transformed into the three-hybrid yeast host strain L40-coat. A root and nodule cDNA library was then introduced into these strains to screen for cDNAs encoding proteins conferring His-independent growth only in the presence of the MS2-*enod40* RNA. Seven clones satisfying all selection criteria corresponded to a protein containing an RRM, which was called MtRBP1. In various subsequent three-hybrid screens, MtRBP1 was repeatedly isolated. No positive clones were found to interact with the MS2-stem RNA.

In the yeast three-hybrid system, MtRBP1 interacts with the full-length *enod40* RNA (Figure 1A) but not with a sequence spanning one of the conserved computationally predicted stems (asterisk in Figure 1C; Sousa et al., 2001). Recently, different regions spanning conserved stems all along the *enod40* RNA have been described using in vitro approaches (Girard et al., 2003) and are indicated in Figure 1C. The isolated cDNA translated in vitro and used in RNA pull down experiments confirmed the interaction of the MtRBP1 protein with the *enod40* RNA (Figure 1B). A fusion protein, glutathione *S*-transferase (GST)-MtRBP1, was expressed in *E. coli* and purified to perform RNA pull down experiments. The fusion protein was also able to bind to the *enod40* RNA in vitro (Figure 1D), and the region of the RNA involved in the interaction was studied. Using different deletions of the *enod40* RNA, we found that both 5′ and 3′ regions of the *enod40* transcript were able to bind GST-MtRBP1 (Figure 1D), whereas the central part of the gene (from nucleotides 110 to 330) did not seem to be involved in the interaction. These results correlated with the interactions observed in yeast and suggested that MtRBP1 bound in vitro to the *enod40* RNA at multiple sites.

MtRBP1 contains one RRM and an Arg/Ser–rich domain at the C terminus as well as an NLS in the N terminus. A phylogenetic

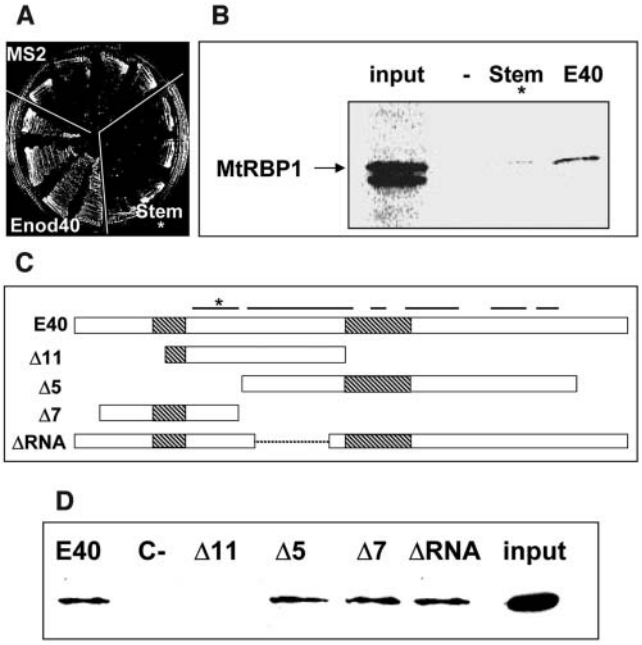

Figure 1. Interaction between MtRBP1 and *enod40* RNA.

(A) The MtRBP1 cDNA was transformed into yeast strains containing RNA-expressing plasmids carrying MS2 repeats only (MS2), an MS2-*enod40* fusion (*enod40*), and an MS2-stem construct (stem *, corresponding to the *enod40* region indicated with an asterisk in **[C]**). Four independent transformants of each strain were plated on selective medium without His.

(B) RNA pull down analysis of stem (*) and *enod40* (E40) RNAs. The input lane contains 20% of translation products used for each binding assay. The lower band may correspond to a subproduct of the in vitro translation of MtRBP1.

(C) Schematic representation of the different regions spanning conserved stem-loops along the *enod40* RNA (lines; Girard et al., 2003). The stem-loop indicated with an asterisk corresponds to the one previously predicted by Sousa et al. (2001). Boxes I and II are indicated as rectangular boxes.

(D) RNA pull down experiments with the GST-MtRBP1 protein purified from *E. coli* and different regions of the *Mtenod40* RNA schematized in **(C)**. C- is a control reaction in which no RNA was included.

tree was constructed from the most related RRM-containing plant proteins with a similar size, and a cluster could be established for the proteins from *M. truncatula*, *G. max*, and Arabidopsis (data not shown). These three sequences share, apart from the RRM domain and the NLS in their N terminus, a conserved 11–amino acid region of unknown function (Figure 2). No metazoan homolog was identified for MtRBP1. Although the RRM domain is widespread from bacteria to humans in a large variety of proteins, no similarities were obtained with the rest of the sequence.

MtRBP1 Is Expressed in Several Tissues of *M. truncatula*

The expression pattern of MtRBP1 was analyzed in different tissues. *MtRBP1* was shown by RNA gel blot analysis to be constitutively expressed in all tissues analyzed; by contrast, as previously found (Crespi et al., 1994), *Mtenod40* was expressed in nodules at a high level, to a lesser extent in stems and roots, and was not detected in leaves (Figure 3A). Semiquantitative RT-PCR analysis from roots and nodules at different developmental stages showed no significant differences in the levels of *MtRBP1* expression, whereas *enod40*, as expected, was induced during nodulation at a high level (Figure 3B). To check for RNA loading, *Mtc27* was used for the RNA gel blot and in the RT-PCR analysis. Transcription of MtRBP1 was not significantly regulated in the tissues studied or during nodule development.

MtRBP1 Localizes in Nuclear Speckles and Is Exported into Cytoplasmic Granules during Nodule Development

Localization of MtRBP1 was initially analyzed using translational fusions to the DsRed2 fluorescent protein. An MtRBP1-DsRed2 fusion protein construct (under the control of the 35S promoter) was introduced into *M. truncatula* roots by *Agrobacterium rhizogenes*–mediated transformation (Boisson-Dernier et al., 2001). Red fluorescence exhibited nuclear speckles in all root cell layers (Figures 4A and 4B), and this protein was not detected in the cytoplasm of these cells (as can be observed at higher magnification in Figure 4B). However, when nodule primordia from the same roots were analyzed, no red fluorescence could be observed in the nucleus of the cells (Figure 4C). On the contrary, some bright red granules corresponding to DsRed2 were observed in the cytoplasm (indicated by an arrow in Figure 4C). Nevertheless, the signals obtained were very weak because of the high levels of autofluorescence in nodule tissues (data not shown). Thus, we could not continue to exploit this method for further analyses of the MtRBP1 localization during nodule development or in mature nodules.

To follow the endogenous MtRBP1 protein during nodulation, antibodies were generated against two synthetic MtRBP1 peptides (see Methods for details) and used in protein gel blot and immunolocalization studies. A protein corresponding to the expected size (~35 kD) could be detected in root and nodule extracts using affinity-purified antibodies (Figure 4D).

In mature indeterminate nodules, several zones can be identified, including the differentiating region (region II) and the nitrogen-fixing region (region III). Cells from the meristematic and differentiating regions accumulate high amounts of the *enod40* RNA, as detected by in situ hybridization (Figure 4E). Immunolocalization studies were then performed in nodule tissues (Figures 4F to 4H) using MtRBP1 antibodies (red channel) in combination with an antibody against tubulin (green channel) to visualize the shape of the cells and 4′,6-diamidino-2-phenylindole (DAPI) staining to detect the cell nuclei (blue channel). Two different subcellular localization patterns were observed for MtRBP1 in different regions of the nodule. In the cells from region III, the protein was exclusively detected in the nucleus, as can be seen in Figures 4F and 4G (coincidence between the red and blue signals, indicated with an arrow in Figure 4G), and completely absent from the cytoplasm. The cytoplasm of cells from region III contains the bacteroids, differentiated bacteria responsible for

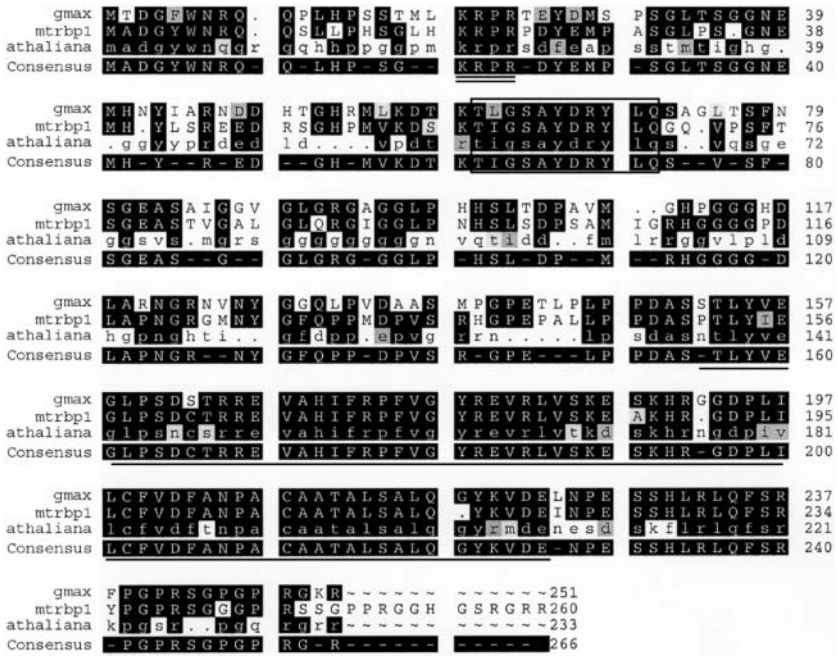

Figure 2. Sequence Analysis of the MtRBP1 Protein.

Alignment of the most related sequences to MtRBP1 from *A. thaliana* and *G. max* and their consensus sequence. The C-terminal RRM domain is underlined, the NLS is underlined twice, and the 11–amino acid domain conserved in the N-terminal region of the three proteins is boxed.

nitrogen fixation. The bacterial DNA explains the presence of a cytoplasmic DAPI signal in these cells. These differentiated nodule cells do not express the *enod40* gene (Figure 4E). By contrast, in the cells from region II (strongly expressing *enod40*), MtRBP1 also could be detected in the cytoplasm (Figures 4G and 4H, cytoplasmic granules indicated by an arrow in 4H). When a single image was obtained from this region, we could clearly observe the accumulation of MtRBP1 in cytoplasmic granules (see the arrow in Figure 4H). The image in Figure 4G corresponds to a snapshot from different sections from the same region, explaining the appearance of the cytoplasm as a continuous line (likely because of the superposition of granule patterns). In the *enod40*-expressing cells from the differentiating region of the nodule, MtRBP1 was specifically localized in the cytoplasm. In the other nodule regions, MtRBP1 remained exclusively nuclear.

The RRM Domain and the N-Terminal Part of MtRBP1 Are Both Required for Exclusive Nuclear Localization

To analyze the different domains of MtRBP1 responsible for its subcellular localization, we continued our studies in *A. cepa* epidermal cells. The MtRBP1-DsRed2 construct was introduced into these cells by biolistics, and 24 h later, the fusion protein could be exclusively observed in nuclear speckles (Figures 5A and 5B) in a similar pattern to that observed in *M. truncatula* roots. No accumulation of the protein could be detected in the cytoplasm of these cells. The DsRed2 control was detected in both the nucleus and the cytoplasm in a diffuse localization (Figure 5A, control). To characterize which part of the protein was responsible for the localization to nuclear speckles, two different constructs containing the N- and C-terminal parts, respectively, of the protein fused to DsRed2 were analyzed (Figures 5B to 5D). The fusion protein containing the N-terminal region carrying the NLS of MtRBP1 (deletion of the RRM domain and the Ser/Arg-rich region) exhibited a diffuse pattern in both nucleus and cytoplasm (cf. Figures 5B and 5C) similar to the DsRed2 protein alone. Fusion proteins containing the RRM domain of MtRBP1 and DsRed2 localized to nuclear and cytoplasmic particles (Figure 5D). These results show that both the C and N termini of MtRBP1 carrying an NLS and a RRM motif, respectively, are required for an exclusive nuclear localization. The RRM domain was sufficient to localize RBP1 in cytoplasmic and nuclear particles, in contrast with the N-terminal fusion that remained diffused. Nevertheless, MtRBP1 was never detected in the cytoplasm in at least 10 different independent experiments.

The Presence of *enod40* in *A. cepa* Cells Induces the Accumulation of MtRBP1 in Cytoplasmic Granules

The immunolocalization experiments showed that the MtRBP1 protein was localized in the cytoplasm in those nodule cells that accumulated *enod40*; however, in the rest of the cells, it remained exclusively nuclear. To investigate whether this relocalization is a direct action of the *enod40* RNA independently of other nodule proteins, we used a heterologous system (epidermal cells of *A. cepa*), where MtRBP1 showed a similar localization to that observed in root cells. We cobombarded two

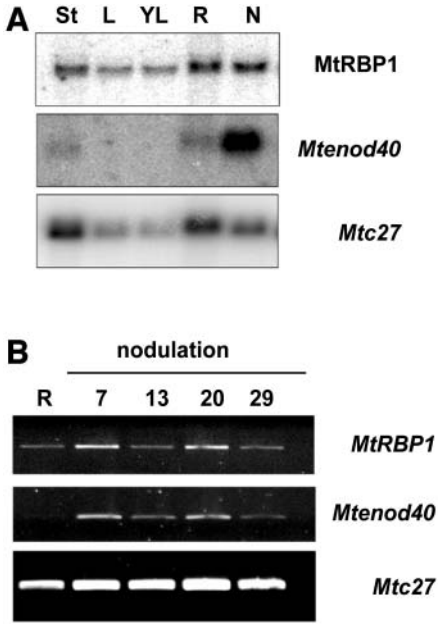

Figure 3. Expression Patterns of *MtRBP1* Transcripts.

(A) RNA gel blot analysis of RNA prepared from stems (St), mature leaves (L), young leaves (YL), roots (R), and nodules (N). Probes are indicated at the right, and *Mtc27* was used as RNA-loading control.

(B) Semiquantitative RT-PCR analysis from roots (R) and nodules at 7, 13, 20, and 29 d after *R. meliloti* infection. The ethidium bromide–stained gel is shown. Specific primers for *MtRBP1* and *Mtenod40* were used, and amplification of *Mtc27* was used as a constitutive control.

different plasmids simultaneously, one containing the fusion protein MtRBP1-DsRed2 as before and another one containing a tandem construction carrying 35S-*enod40* and 35S-GFP (green fluorescent protein) transgenes. As negative control, cobombardment of the MtRBP1-DsRed2 fusion with a plasmid containing only a 35S-GFP was analyzed. Both plasmids were present in all transformed cells, indicating a 100% efficiency of cobombardment. As shown in Figure 6, coexpression of GFP (as marker of the *enod40* plasmid) and the MtRBP1-DsRED2 protein in the same cell showed nuclear and cytoplasmic red fluorescence in ~50% of the cells. MtRBP1 was exclusively nuclear in the absence of the *enod40* transgene, either when cobombarded with the GFP control (Figure 6B; representative result from five independent experiments) or alone (Figures 5A and 5B). These results indicate that coexpression of the *enod40* RNA seems sufficient to induce MtRBP1 accumulation in the cytoplasm. Two mutant *enod40* transcripts, in which the ATG in sORFI or sORFII (spanning Boxes I and II, respectively) has been replaced by an ACG, were obtained by site-directed mutagenesis from the plasmid 35S-*enod40*:35S-GFP. When each of these transcripts was cointroduced with MtRBP1-DsRed2 in *A. cepa* cells, red fluorescence could be observed in the cytoplasm of cobombarded cells at a similar frequency as before. No difference could be observed between these transcripts and the wild-type *enod40* transcript concerning their ability to relocalize MtRBP1 (data not shown). The fact that ATG mutants that disrupt the translation of the *enod40*-encoded peptides were still able to induce the cytoplasmic localization of MtRBP1 strongly suggests that the *enod40* RNA itself is responsible for this activity.

The *enod40* RNA Accumulates in Nuclear and Cytoplasmic Particles in Living Plant Cells

The next question to address was whether the *enod40* RNA is directly associated to MtRBP1 in the cytoplasm. To answer this question, we developed an in vivo approach allowing us to visualize the RNA in living cells. An elegant method based on the use of the GFP as a reporter has been successfully used to follow specific mRNAs in living yeast cells (Bertrand et al., 1998) and in cultured rat hippocampal neurons (Rook et al., 2000). The DNA sequence of the RNA to be traced was fused to a sequence encoding various copies of the MS2-RNA, and in parallel, the MS2-coat protein is fused to the GFP. By cointroducing both constructs into a living cell, the RNA of interest could be detected through the binding of the MS2coat-GFP protein to the MS2-RNA tags. Interaction between an MS2coat-GFP fusion protein and an *enod40* RNA construct tagged with two MS2 RNA binding sites allowed us to localize the *enod40* transcript in living plant cells. Both constructs were introduced into *A. cepa* epidermal cells (as mentioned before, 100% efficiency of cobombardment was observed in our conditions). Confocal microscopy revealed that GFP fluorescence accumulated in bright cytoplasmic and nuclear granules in ~60% of cells harboring both constructs (Figures 7A to 7C), whereas the MS2coat-GFP fusion alone exhibited a diffuse pattern in both compartments (Figures 7D to 7F). Similar patterns of GFP fluorescence were observed for two other RNAs (data not shown): *Mtapk1*, which encodes a protein kinase (1700 bp; Chinchilla et al., 2003), and del-*Mtapk1*, which is a deleted version of *Mtapk1* of the same size as *enod40* (600 bp). Hence, the observed distribution of MS2-GFP was dependent on the presence of an RNA, validating this methodology for plant cells. No specific localization could be observed for the *enod40* RNA as compared with the other RNAs used in our experiments.

The *enod40* RNA Colocalize with MtRBP1 into Cytoplasmic Granules

To monitor the association between MtRBP1 and the *enod40* RNA in vivo, we introduced three plasmids carrying the MtRBP1-DsRed2, MS2-*enod40* RNA, and MS2coat-GFP constructs into the same cell. Triple-transformed cells showing red and green fluorescence, the latter exhibiting a pattern typical for RNA (as seen in Figure 7A), were further analyzed. Interestingly, in the presence of the MS2-*enod40* RNA (green fluorescence), the MtRBP1 fusion protein (red fluorescence) was detected in bright cytoplasmic granules (see detail presented in Figure 8A) as well as in nuclear speckles in ~50% of the cells. Other RNAs tested (*Mtapk1* is presented as an example in Figure 8B) did not induce any change in the nuclear localization of MtRBP1-DsRed2, although nuclear and cytoplasmic green granules could be detected (indicating the presence of the hybrid RNA molecules in the cells). In addition, a diffuse pattern was observed for MS2coat-GFP, in the absence of hybrid RNA, both in cytoplasm

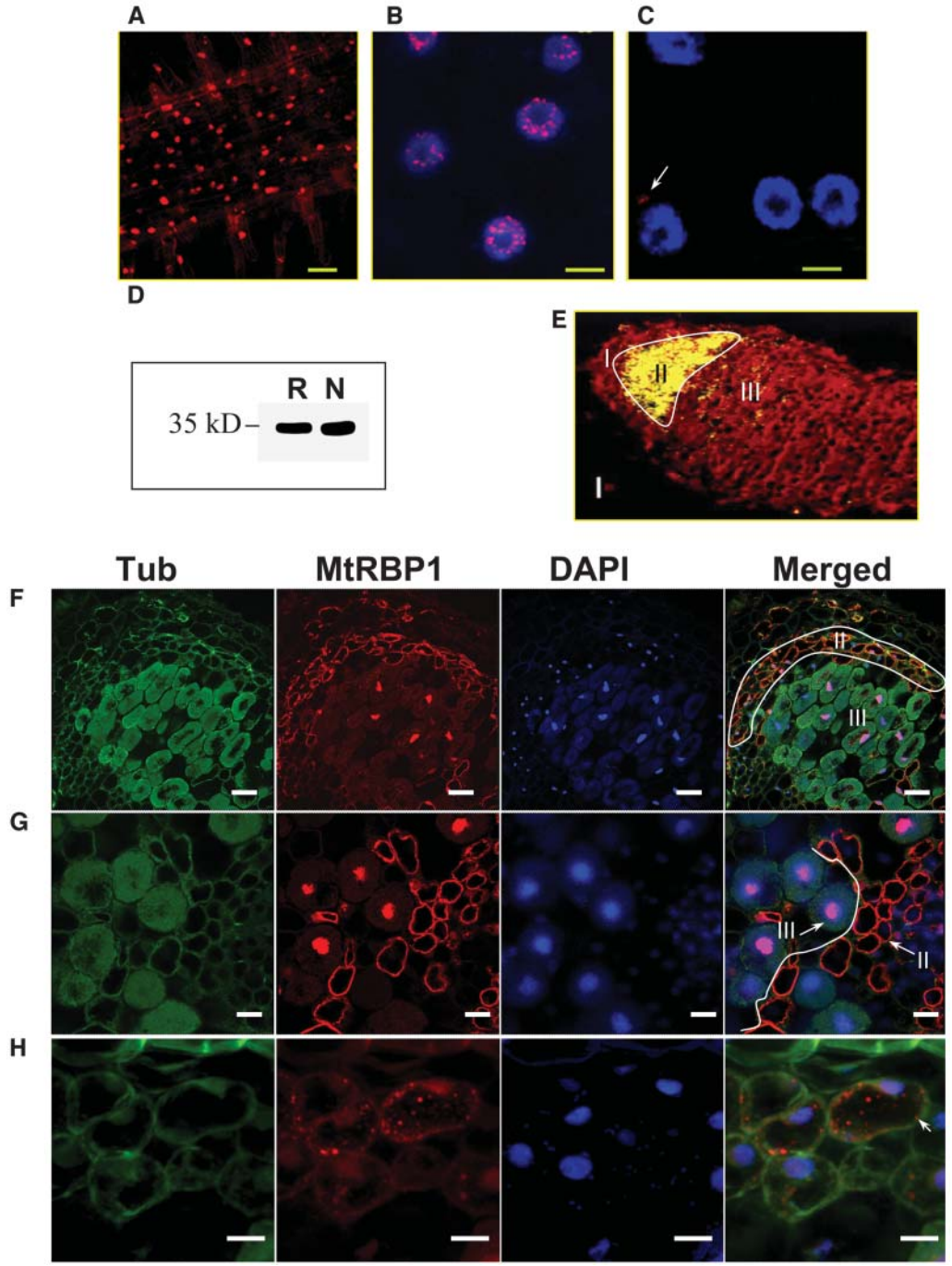

Figure 4. MtRBP1 Localization in *M. truncatula* Roots and Nodules.

(A) Confocal image of a root, showing accumulation of red fluorescence in the nucleus of all cells. The laser intensity was increased to visualize root shape. Scale bar = 40 μm.

(B) Detail of root cells showing accumulation of MtRBP1-DsRed2 in nuclear speckles.

(C) Less or no red fluorescence was observed in the nuclei of nodule primordium cells. Some bright granules could be observed outside the nucleus (indicated by an arrow). Nuclei were stained with DAPI in **(B)** and **(C)**. The three images correspond to the same nodulated root. Scale bars in **(B)** and **(C)** = 8 μm.

(D) Protein gel blot analysis revealed that anti-MtRBP1 antibodies recognized a band of 35 kD on protein extracts from roots (R) and nodules (N).

(E) *enod40* in situ hybridization in a mature nodule longitudinal section; the different nodule regions are indicated: I, meristem; II, invasion zone (differentiating cells); and III, nitrogen-fixing zone or symbiotic zone. Yellow color indicates the accumulation of *enod40* transcripts. The region where *enod40* transcripts accumulate is shown in white.

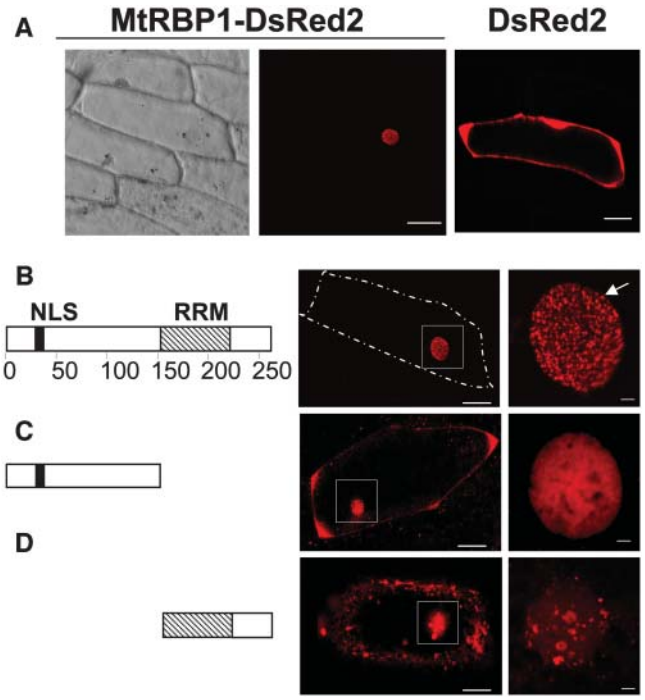

Figure 5. Subcellular Localization of MtRBP1-DsRed2 Fusion Protein in *A. cepa* Cells.

(A) Localization pattern observed for MtRBP1-DsRed2 fusion protein. Left panel, Nomarski image; middle panel, red fluorescence. Compare with the pattern observed for the DsRed2 control, diffused both in the nucleus and in the cytoplasm. Scale bars = 40 μm.

(B) to **(D)** Localizations observed for the different MtRBP1 deletions fused to the DsRed2. Scale bars = 40 μm in left panels and 20 μm in right panels.

(B) Entire MtRBP1 protein; the shape of the cell is outlined by a dashed line. Nuclear speckles are indicated by an arrow in the right panel.

(C) Fusion protein containing the N-terminal region carrying the NLS of MtRBP1.

(D) Fusion protein containing the RRM domain and the Ser/Gly-rich region of MtRBP1. Images corresponding to the entire cell (left panels) and to a magnification of the nucleus (right panels) are presented in **(B)**, **(C)**, and **(D)**.

and nucleus, as expected, and no MtRBP1 could be detected in the cytoplasm of these cells (Figure 8C).

The spectral profiles of the GFP and DsRed2 fluorochromes were analyzed in the cytoplasm of five cells containing both MtRBP1 and *enod40*, which indicated that the *enod40* RNA and MtRBP1 protein colocalized in the cytoplasmic granules (as shown for one cell in Figure 8D). In some cells, we could follow the movement of both the *enod40* RNA and MtRBP1 from the nucleus into the cytoplasm, suggesting that *enod40* interacts with MtRBP1 in the nucleus and is associated with this protein at all stages of transit. Furthermore, when the protein was detected in the cytoplasm, it was always associated with the RNA (Figure 8D; data not shown), whereas the RNA molecules were not always associated with the protein (arrow in Figure 8D). This indicated that, to accumulate into the cytoplasm, MtRBP1 needs to be associated to the *enod40* RNA.

DISCUSSION

In this work, we described a new function for the *enod40* RNA during nodule development. First, a novel RBP, MtRBP1, has been identified to interact with *enod40*. Then it was shown that in mature nodules, the localization of MtRBP1 was cytoplasmic in those cells expressing the *enod40* gene at high levels, whereas it was found in the nucleus in the rest of the cells. Evidence for the direct implication of the *enod40* RNA in this relocalization results from the utilization of a heterologous system, where MtRBP1 was exclusively localized in the nucleus. When *enod40* was coexpressed in these cells, and only in that case, the protein could be detected in the cytoplasm. The *enod40*-encoded peptides do not seem to be involved in this activity because mutant *enod40* genes where the ATG was replaced by an ACG were still able to induce the cytoplasmic localization of MtRBP1. Finally, a direct association between the RNA and the protein was demonstrated using a methodology specially aimed at following both molecules in living cells. Hence, the RNA itself but not the encoded peptides seems to be responsible for this activity.

Using the yeast three-hybrid system, an RBP, MtRBP1, has been identified to interact with the *enod40* RNA. Despite the high levels of conservation for the stem and loop structure predicted between the two conserved boxes (Sousa et al., 2001; Figure 1C), this region does not seem responsible for the interaction with MtRBP1. When we started our study, this was the only predicted stem-loop in the *enod40* transcript. Recently, other highly structured stem-loops through the *enod40* RNA molecule have been identified (Girard et al., 2003). It would be of great interest to analyze which of them is responsible for the interaction with MtRBP1. RNA pull down experiments allowed us to confirm the interaction of this protein with *enod40* RNA but not with this predicted stem-loop (Figure 1B). It has been shown that both 5′ and 3′ regions, containing the conserved Box I and Box II, are able to elicit cell-specific growth responses in the *M. sativa* root cortex (Sousa et al., 2001). Both regions (corresponding to constructs Δ5 and Δ7 in Figures 1C and 1D) also are able to

Figure 4. (continued).

(F) to **(H)** Immunological studies in mature nodules: anti-tubulin (green channel) (Tub), anti-MtRBP1 (red channel), DAPI staining (blue channel), and the merged image are presented.

(F) General view of a mature nodule; the regions II and III are indicated. Scale bars = 40 μm.

(G) Higher magnification allowing a better comparison for the different subcellular localization of MtRBP1 in the cells from regions II and III; the separation between regions II and III is indicated with a line. Scale bars = 20 μm.

(H) Details from region II cells. Single scan image of a cell in region II; MtRBP1 can be detected in cytoplasmic granules (arrow). Scale bars = 10 μm.

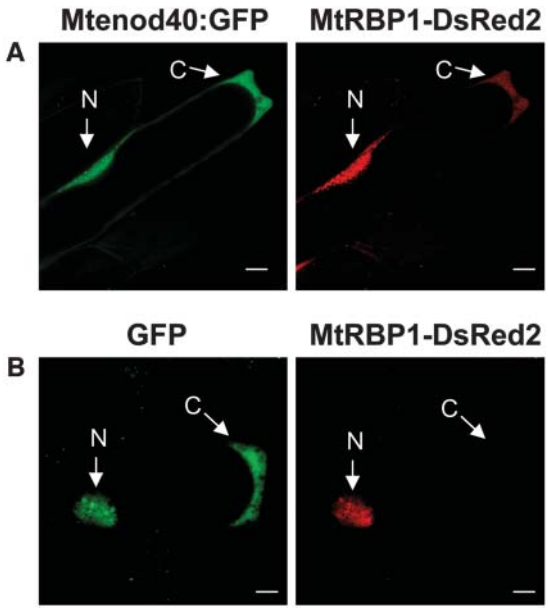

Figure 6. MtRBP1 Accumulates in the Cytoplasm in the Presence of the *enod40* RNA.

(A) Cobombardment of 35S-MtRBP1-DsRed2 and 35S-*enod40*:35S-GFP.
(B) Cobombardment of 35S-MtRBP1-DsRed2 and 35S-GFP.
N, nucleus; C, cytoplasm. Scale bars = 20 μm.

interact with MtRBP1. By contrast, a deletion of the inter-ORF region, which was shown to reduce the biological activity of the *enod40* gene (Sousa et al., 2001) does not seem to affect the binding of the RNA to the MtRBP1 protein (ΔRNA in Figures 1C and 1D). Nevertheless, it is difficult to predict how a deletion in a gene will disrupt the RNA structure. At present, we cannot correlate biological activity with specific stem-loops of the *enod40* RNA.

Many different RNA binding motifs have been identified, and one of the most widely spread is the RRM or RNP motif (Burd and Dreyfuss, 1994). A computer search in the Arabidopsis genome revealed 196 different RRM-containing proteins, suggesting a higher complexity of this family of proteins in plants than in metazoa (Lorkovic and Barta, 2002). Several proteins containing similar RRM domains and of similar size to MtRBP1 have been identified in the plant kingdom, and two of them, from Arabidopsis and *G. max*, share with MtRBP1 a potential NLS in the N terminus and a common 11–amino acid region of unknown function. It would be interesting to investigate whether these proteins change their localization during specific developmental stages through interaction with *enod40* or other sORF-mRNAs (no *enod40* homolog has been found in Arabidopsis).

In situ hybridization studies in mature nodules have revealed that *enod40* RNA is accumulated at very high levels in the differentiating cells from region II (Crespi et al., 1994). Once the cells are invaded by *Rhizobium meliloti*, they enlarge and differentiate into cells of the symbiosis zone (zone III) where transcripts for *enod40* are no longer detected (Crespi et al., 1994). In our immunolocalization experiments, we observed a different subcellular localization for MtRBP1 in these two different nodule regions. Interestingly, in the cells expressing *enod40*, the protein appears to be localized in the cytoplasm, whereas it is restricted to the nucleus in the rest of the cells. The clear correlation that can be established between the expression of *enod40* and the cytoplasmic localization of MtRBP1 in the different nodule regions suggests that *enod40* affects MtRBP1

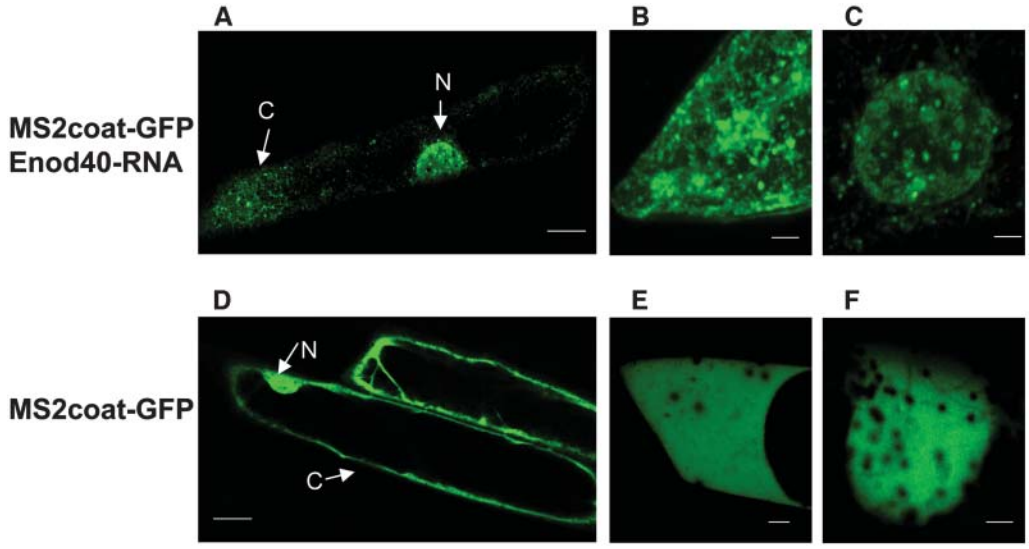

Figure 7. Localization of *enod40* RNA in *A. cepa* Cells.

(A) to **(C)** Cells bombarded with the MS2-*enod40* hybrid RNA and the MS2coat-GFP protein showed green fluorescence accumulating in cytoplasmic (detail in **[B]**) and nuclear **(C)** fluorescent granules.
(D) to **(F)** Introduction of the MS2coat-GFP fusion alone into the cells resulted in a diffuse GFP pattern both in the cytoplasm **(E)** and the nucleus **(F)**.
N, nucleus; C, cytoplasm. Scale bars = 20 μm in top panels and 5 μm in bottom panels.

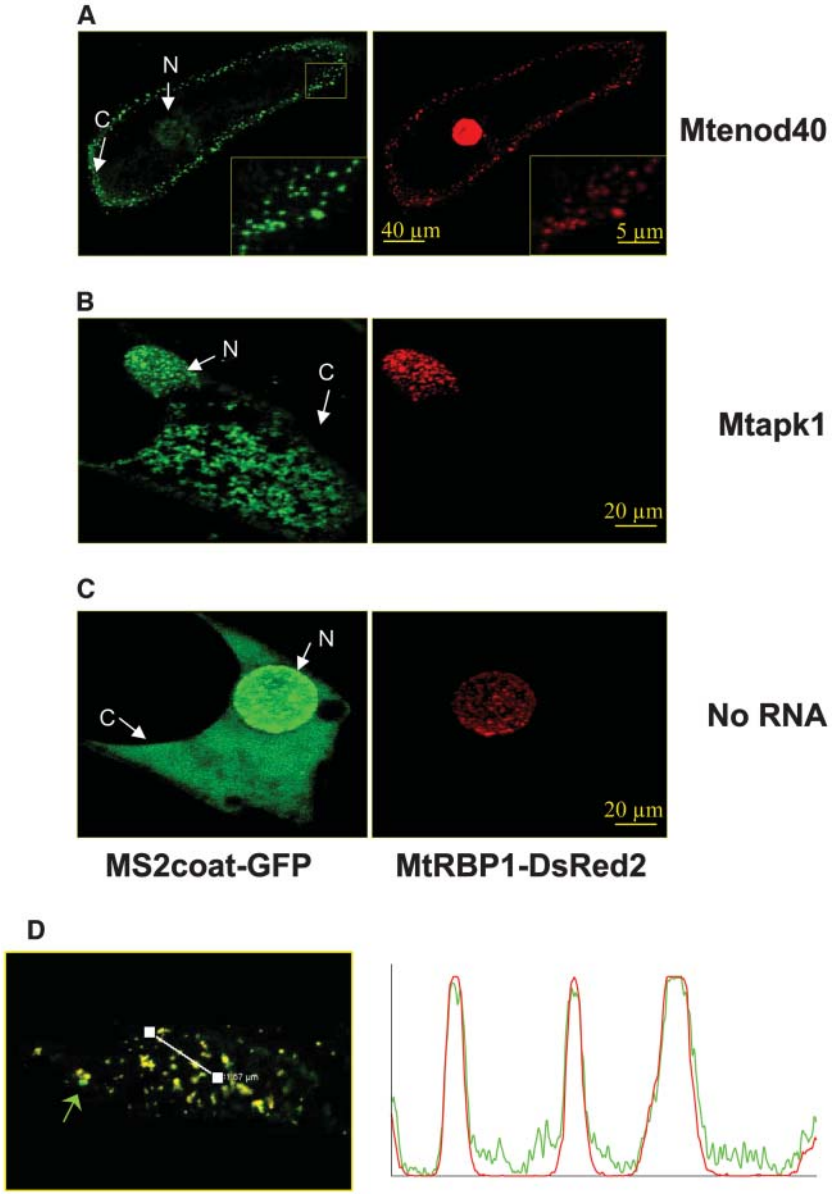

Figure 8. Cytoplasmic Localization of MtRBP1 in the Presence of the *enod40* RNA.

(A) to **(C)** Cobombardments with MS2coat-GFP, MtRBP1-DsRed2, and the following MS2-RNA constructs: MS2-*enod40* RNA (600 nucleotides) **(A)**, MS2-*Mtapk1* RNA (1700 nucleotides) **(B)**, and no hybrid RNA **(C)**. Cells were observed for GFP and DsRed2 fluorescence, which label hybrid MS2-RNA molecules and the MtRBP1 protein, respectively. Note that red fluorescence can be detected in cytoplasmic granules only in the presence of *enod40* (top right panel). N, nucleus; C, cytoplasm. Scale bars are indicated.

(D) Cobombardment of MtRBP1-DsRed2, MS2coat-GFP, and MS2-*enod40* RNA. Detail of a merged image of the cytoplasm with the corresponding spectral fluorescence profile (obtained along the indicated white line in the image), showing colocalization between the *enod40* RNA (green) and the MtRBP1 protein (red). The arrow indicates the presence of *enod40* RNA (green) not associated to MtRBP1 (red) in the cytoplasm. Note that all granules are green or yellow but never red (MtRBP1 alone was not detected in the cytoplasm).

localization during nodule development, changing its localization from the nucleus to the cytoplasm. The fact that MtRBP1 and *enod40* are not exclusively expressed during nodulation suggests that the cytoplasmic localization of MtRBP1 also occurs in other cells from the plant. It will be very interesting to investigate the localization of MtRBP1 in the cytoplasm of other cells expressing *enod40* as well as the localization in different tissues or developmental stages of the MtRBP1-related proteins identified in *G. max* and Arabidopsis. In the different root tissues (pericycle, endodermis, cortex, and epidermis), MtRBP1 was exclusively detected in the nuclei of *M. truncatula* cells. The fact that we can reproduce MtRBP1 relocalization in the

heterologous system by overexpressing at the same time MtRBP1 and *enod40* suggests that there are no other specific proteins or RNAs required for that activity. However, it is likely that other proteins participate in this relocalization process in the nodule and/or interact with the complex, perhaps increasing the efficiency of MtRBP1 accumulation in the cytoplasm.

A similar regulation has been described for the SR proteins during the *Ascaris lumbricoides* embryogenesis. As development proceeds, the nuclear amounts of SR proteins increase while the protein levels in the cytoplasm decreases (Sanford and Bruzik, 2001). In plants, the subcellular localization of RBPs also can be modulated by external environmental conditions, as the subnuclear reorganization of AKIP1 (a nuclear RBP) in response to the plant hormone abscisic acid (Li et al., 2002). Nucleocytoplasmic macromolecular transport complexes, containing mRNAs and proteins, have been described in many biological systems (Arn and Macdonald, 1998). Several proteins and/or RNAs are probably involved in the formation of the MtRBP1-containing ribonucleoparticles that we could observe as cytoplasmic granules in immunolocalization and the transient expression experiments. Many RBPs turn out to have multiple regulatory functions in different cellular compartments, providing links between different aspects of RNA metabolism in the nucleus and the cytoplasm (Dreyfuss et al., 2002).

MtRBP1 was detected in a speckled localization pattern in *M. truncatula* roots and in *A. cepa* cells. Several RBPs localize to nuclear speckles (e.g., SR proteins; Cáceres et al., 1998). These intrachromatin granule clusters have been implicated in transcription and mRNA processing, and their distribution, size, and abundance depend on cellular transcriptional activity. MtRBP1 seems to be very efficiently transported into the nucleus after translation, and not only the NLS seems to be responsible for that because a truncated version of the protein containing the NLS also is detected in the cytoplasm. The RRM domain alone has the ability to direct the protein to nuclear speckles as well as to cytoplasmic granules. These observations reinforce the idea that protein localization to nuclear speckles does not rely on a simple targeting motif but is more complex and probably involves phosphorylation and protein–protein interactions as shown for other RBPs (Cáceres et al., 1998).

The heterologous *A. cepa* cell system allowed us to demonstrate that the MtRBP1 subcellular localization that we observe during nodule development was a direct effect of the *enod40* RNA. Most of the proteins whose activities are regulated by transport into different subcellular compartments are in fact continuously shuttling between nucleus and cytoplasm (Shyu and Wilkinson, 2000; Gama-Carvalho and Carmo-Fonseca, 2001). Shuttling proteins typically have both an NLS and a nuclear export signal. The fact that only an NLS sequence (and no nuclear export signal) has been identified in the MtRBP1 sequence and that we have never detected MtRBP1 in the cytoplasm unless associated to the *enod40* RNA allows us to propose that MtRBP1 is not a shuttling protein but requires binding to *enod40* RNA to accumulate in the cytoplasm.

Highly sensitive methods have been developed recently for detecting RNA movement and localization in living cells. These approaches include microinjection of fluorescent RNA, in vivo hybridization of fluorescent oligonucleotides, and expression of fluorescent RBPs (Dirks et al., 2001; Pederson, 2001). Indirect labeling of mRNAs with GFP has been successfully applied in yeast cells and rat neurons (Bertrand et al., 1998; Rook et al., 2000). This methodology allowed us to follow the accumulation of different RNAs in plant cells, and a particulate localization was observed in both the nucleus and the cytoplasm for all RNAs tested. Although nuclear speckles have been primarily implicated in splicing (Melcak et al., 2001), these intranuclear sites also have been associated with the transcription of abundantly expressed genes (Zeng et al., 1997). All the RNAs studied were strongly expressed, which could explain their localization in nuclear speckles even if they are not spliced.

In the immunolocalization experiments, we have seen that MtRBP1 was localized in the cytoplasm exclusively in the nodule cells expressing *enod40*. Using the indirect labeling of RNAs with MS2 tags, we determined that both *enod40* and MtRBP1 colocalized in the same cytoplasmic granules. Because we have never detected the protein alone in these particles, MtRBP1 seems to require the association with the *enod40* RNA to accumulate in cytoplasmic granules. Another sORF-mRNA implicated in nucleocytoplasmic transport has been found in yeast. The meiRNA promotes meiosis I by facilitating the nuclear localization of the RBP Mei2 (Yamashita et al., 1998; Sato et al., 2001). This methodology used to monitor RNA–protein interactions in a living cell can be applied to other biological processes involving similar macromolecular interactions.

Our results suggest that a sORF-mRNA, *enod40*, mediates the cytoplasmic relocalization of a nuclear RBP, MtRBP1. We speculate that modification of the subcellular localization of RBPs may represent a novel RNA function in the cell.

METHODS

Plant Material and Bacterial Strains

Seeds of *M. truncatula* cultivar R108 were sterilized for 30 min (7 g/L Bayrochlor; BAYROL, Planegg, Germany) and rinsed four times in sterile water. Plants were grown under a 16-h photoperiod and 25°C and 15°C for day and night, respectively, and inoculated with *Sinorhizobium meliloti* Rm41 as described (Crespi et al., 1994).

E. coli DH5α (*supE44*, *hsdR17*, *recA1*, *endA1*, *gyrA96*, *thi-1*, and *relA1*) was used for subcloning. *E. coli* strain BL21 [F-, *omp*T, *hsd*S_B (r_B-, m_B-), *dcm*, *gal*, λ(DE3), pLysS, and Cm^r] was used for the production of GST-MtRBP1. The yeast strain L40-coat [*MATa*, *ura3-52*, *leu2-3*, *112*, *his3Δ200*, *trp1Δ1*, *ade2*, *LYS2*::(*LexA op*)$_4$-*HIS3*, *ura3*::(*LexA op*)$_8$-*lacZ*, and *LexA-MS2 coat* (*TRP1*)], auxotrophic for uracil, Leu, adenine, and His, was used for the three-hybrid screenings (Sengupta et al., 1996).

Three-Hybrid Screening

The components for the three-hybrid system were kindly provided by M. Wickens, and *HIS3* and *lacZ* served as reporter genes (Sengupta et al., 1996). The full-length *Mtenod40* cDNA and a region (nucleotides 142 to 215) spanning one of the predicted RNA stem-loops (Sousa et al., 2001) were introduced into the unique *Sma*I site of the vector pIII/MS2-1, containing URA3. These constructs, pIII/MS2-*enod40* and pIII/MS2-stem, were transformed into the yeast strain L40-coat (Sengupta et al., 1996). The yeast strains were then transformed with a *M. truncatula* cDNA library (Gyorgyey et al., 2000), and transformants were selected on

media lacking Leu and His and containing 5 mM 3-aminotriazole. To eliminate false positives growing independently of RNA, transformants were not selected for the maintenance of the RNA plasmid. As expected, false positives that did not require the RNA to activate HIS3 lost the RNA plasmid and the ability to grow in a medium without uracil. In fact, 35 out of 73 transformants grew independently of the RNA. To further refine the screening, the remaining 28 colonies were treated with 5-fluoroorotic acid to cure the RNA plasmid. Sixteen more clones were discarded (able to grow without His even in the absence of RNA). Seven of the twelve cDNA clones meeting all selection criteria corresponded to MtRBP1. Two subsequent screens performed in a similar way (but without the 5-fluoroorotic acid treatment) also yield MtRBP1 repeatedly.

Plasmid Construction

For in vitro transcription, constructions were done in the plasmid pBluescript pSK+. *Mtenod40* full-length cDNA was cloned into the *Eco*RI/*Xho*I sites, and *Mtenod40*-Δ*5* (nucleotides 204 to 614), *Mtenod40*-Δ*7* (nucleotides 31 to 200), and *Mtenod40*-Δ*11* (nucleotides 110 to 330) were amplified by PCR from the pSK-*Mtenod40* (as previously described in Sousa et al., 2001); in *Mtenod40*-Δ*RNA*, nucleotides 221 to 311 were deleted from the pSK-*Mtenod40*.

For the translational fusions of MtRBP1 to DsRed2, the pPk100 plasmid (gift of Patrick Gallois, University of Manchester, UK), containing the GFP under the control of a double 35S promoter, was used. The DsRed2 (CLONTECH, Palo Alto, CA) was cloned in the *Nco*I/*Not*I sites, replacing the GFP. The *Nco*I in the DsRed2 sequence was previously eliminated by site directed mutagenesis using the oligonucleotides 5′-GCAGAAGAAGACGATGGGCTGGGAGGCCTCC-3′ and 5′-GGAGGCCTCCCAGCCCATCGTCTTCTTCTGC-3′. MtRBP1 was amplified by PCR using the oligonucleotides 5′-CCGGAATTCGATGGCAGATGGCTACTGG-3′ and 5′-AGGCCATGGTTCTTGGACCACCTCCACTTC-3′, containing restriction sites for *Eco*RI and *Nco*I, respectively. Cloning into the *Eco*RI/*Nco*I sites of the vector resulted in an N-terminal fusion to DsRed2. For the deleted versions of MtRBP1, the N-terminal part of the protein was amplified using the oligonucleotides 5′-CCGGAATTCGATGGCAGATGGCTACTGG-3′ and 5′-GGCCCATGGCAGGTCCATGCCTGGAAAC-3′, containing *Eco*RI and *Nco*I restriction sites, respectively, and cloned into the *Eco*RI/*Nco*I sites of the new DsRed2-replaced vector. The C-terminal part of MtRBP1 containing the RRM domain and the Arg/Ser-rich domain was amplified using the oligonucleotides 5′-CCGGAATTC*ATG*CCAACTCTATATATTGAAGG-3′ (an ATG was included to allow the initiation of translation) and 5′-AGGCCATGGTTCTTGGACCACCTCCACTTC-3′ (containing the *Eco*RI/*Nco*I restriction sites for cloning as before). The construct MtRBP1-DsRed2 was cloned into the binary vector pCP60 (Charon et al., 1999) for the generation of transgenic roots.

For the RNA pull down experiments, MtRBP1 was fused to the GST by PCR amplification using the oligonucleotides 5′-CCGGAATTCGATGGCAGATGGCTACTGG-3′ and 5′-TAGTCTAGACTACTTCTTGGACCACCTCCACTTC-3′, containing the *Eco*RI and *Xba*I sites, respectively, and cloned into the *Eco*RI/*Xba*I sites of the pGex-2T plasmid.

The construction 35S-*enod40*:35S-GFP was obtained as follows. *Enod40* was first cloned into the *Bam*HI site of the pDH51 plasmid (Sousa et al., 2001) that contains a 35S promoter. The fragment containing the 35S promoter and the *enod40* sequence was transferred into the *Eco*RI site of the pBIN35S-mGFP4 plasmid (Haseloff and Amos, 1995). Two *enod40* mutant transcripts were obtained by site directed mutagenesis, in which the ATG spanning Box I and Box II were replaced by an ACG, disrupting the translation of the encoded peptides.

Constructions for in vivo localization of RNA were done as follows: the fusion MS2-*enod40* was amplified by PCR from the vector pIII/MS2-*enod40*, using the oligonucleotides 5′-CGGGATCCCAAAACATGAGGATCACCC-3′ and 5′-CCGCTCGAGCAGAAACTGAAACAAGAAC-3′, containing the restriction sites *Bam*HI and *Xho*I, respectively, and cloned into the *Bam*HI/*Sal*I sites of the pDH51 vector (Sousa et al., 2001) under the control of the 35S promoter of *Cauliflower mosaic virus*. The full-length RNA (1700 nucleotides) coding for the protein kinase *Mtapk1* (Chinchilla et al., 2003) was amplified by PCR using the oligonucleotides 5′-TCCCCCGGGGAACATGAGGATCACCCATGTCTGCAGGTCGACTCTAGAAAACATGAGGATCACCCATGTCTGGCACGAGATTCCCATGCCTCG-3′ (containing two copies of the MS2 sequence) and 5′-ACGCATGCATGAACGGCGTTGGAGCTGTGGG-3′ (containing *Sma*I and *Sph*I sites, respectively, to clone into the *Sma*I/*Sph*I sites of the pDH51 plasmid). The oligonucleotide containing two copies of the MS2 sequence was used for the amplification of a fragment of 600 nucleotides of the *Mtapk1* RNA, in combination with the oligonucleotide 5′-ACGCATGCATCAGGAACTTCACGAGGATTGC-3′, and cloned into pDH51 following the same strategy. The MS2-coat sequence was amplified by PCR from the yeast strain L40-coat (Sengupta et al., 1996) using the oligonucleotides 5′-CTCTAGAGAATGGCTTCTAACTTTACTCAG-3′ and 5′-CGGGATCCAGTAGATGCCGGAGTTTGC-3′, containing the restriction sites *Xba*I and *Bam*HI, respectively, and cloned as a translational fusion to mGFP4 in pBIN 35S-mGFP4 (Haseloff and Amos, 1995).

RNA Gel Blot Analysis

Total RNA (10 μg) from several tissues was subjected to RNA gel blot analysis by hybridization with ^{32}P-labeled probes corresponding to full-length MtRBP1 or *Mtenod40* as previously described (Sousa et al., 2001). The gene *Mtc27* expressing constitutively in several *M. truncatula* tissues was used as a loading control (Crespi et al., 1994).

RT-PCR

Total RNA was prepared from roots and nodules at different developmental stages and used for reverse transcription using SuperScript II (Invitrogen, Carlsbad, CA) after removing contaminating DNA by DNase treatment (RNase-free DNase from Promega, Madison, WI), as recommended by the manufacturer. *Mtc27* was used as a constitutive control (Crespi et al., 1994). PCR was performed using gene-specific primers for *enod40* forward (5′-TGGCAAACCGGCAAGTCAC-3′) and reverse (5′-CAGAAACTGAAACAAGAAC-3′), for MtRBP1 forward (5′-ATGGCAGATGGCTACTGG-3′) and reverse (5′-CAGGTCCATGCCTGGAAAC-3′), and for *Mtc27* forward (5′-GGGAGGTTGAGGGAAAGTGG-3′) and reverse (5′-CCAAATCATAGTCTCAACTCTCG-3′) used as RNA-loading control. The amplification was as follows: one cycle of 2 min at 94°C, 25 cycles of 30 s at 94°C, 30 s at 60°C, and 1 min at 72°C. The PCR products were analyzed on 1% agarose gels.

GST-MtRBP1 Expression and Purification

The GST-MtRBP1 construct was transformed into *E. coli* strain BL21. A single colony was inoculated into 10 mL of Luria-Broth–ampicillin (100 μg/mL), and the culture was grown overnight at 37°C and used to inoculate 200 mL of Luria-Broth–ampicillin. The culture was grown to an OD_{600} of 0.6 to 0.7. Cultures were induced with 1 mM isopropyl-β-D-thiogalactopyranoside and incubated at 37°C for an additional 4 h. Cells were harvested by centrifugation and resuspended in 1× PBS containing 10 μg/mL of chymostatin, 10 μg/mL of leupeptin, 10 μg/mL of antipapain, and 10 μg/mL of pepstatin A. Extracts were ground with one volume of alumina, and the soluble fraction recovered after centrifugation at 12,000 rpm for 15 min at 4°C. GST-MtRBP1 was batch purified using Glutathione Sepharose 4B according to the supplier's (Amersham Pharmacia Biotech, Uppsala, Sweden) recommendations.

RNA Pull Down Assay

The *enod40* cDNA was amplified by PCR from pSK-*Mtenod40*, using the oligonucleotides T3 (5′-ATTAACCCTCACTAAAGG-3′) and Mar6 (5′-CAGAAACTGAAACAAGAAC-3′) at the 3′ end of *Mtenod40* (Crespi et al., 1994). For the other RNAs, the oligonucleotides T3 and T7 were used for PCR amplification. The PCR product was used for in vitro transcription in the presence of biotinylated-UTP. The biotinylated RNAs were bound to streptavidin-magnetic beads (μMACS Streptavidin kit; Miltenyi Biotec, Bergisch Gladbach, Germany) and incubated with in vitro–translated MtRBP1, or with the fusion protein GST-MtRBP1, for 1 h at 4°C in a buffer containing 10 mM Hepes, pH 7.0, 50 mM KCl, 10% glycerol, 1 mM EDTA, 1 mM DTT, 0.5% Triton X-100, and 0.15 μg/mL of yeast t-RNA and RNase inhibitor. After washing according to the manufacturer's instructions, bound proteins were eluted in Laemmli buffer and resolved by SDS-PAGE, dried, and autoradiographed.

M. truncatula Root Transformation

The binary vector pCP60 (Charon et al., 1999) containing the construct MtRBP1-DsRed2 was introduced into *A. rhizogenes* by electroporation. This *A. rhizogenes* strain was used to transform *M. truncatula* Jemalong seedlings to obtain transgenic roots that were nodulated, essentially as described (Boisson-Dernier et al., 2001).

Antibodies and Immunostaining

Antibodies against MtRBP1 were produced by Eurogentec (Seraing, Belgium) with the Double XP program. Two predicted immunogenic peptides of MtRBP1 were synthesized and coupled to the carrier protein KLH (SGLHKRPRPDYEMPAS [P1] and LSREEDRSGHPMV [P2]). Two rabbits were immunized with a mix of the two coupled peptides, and serums were affinity purified separately against each peptide. Affinity-purified antibodies against P2 yield no signals in protein gel blot analysis. Antibodies purified against P1 gave a specific band of the expected size (dilution 1:1000) and were used in all subsequent experiments. For the immunolocalization studies, nodules were mounted on 6% agarose, and slices of ~100 μm were obtained using the Vibratome MICRO-CUT H1200 (Bio-Rad Microsciences, Paris, France). Nonspecific binding sites were blocked with 5% BSA in MPBS (1× PBS, 10 mM $MgSO_4$, and 10 mM EGTA, pH 6.8) for 1 h at root temperature, and the slices were then incubated overnight at 4°C in the presence of anti-MtRBP1 and anti-tubulin (mouse-monoclonal antibodies from Sigma, St. Louis, MO) antibodies at a 1:1000 dilution. The slices were washed four times during 10 min in MPBS and incubated in the secondary antibodies anti-mouse Alexa Fluor 488 and anti-rabbit Alexa Fluor 568 at a 1:1000 dilution for 1 h at room temperature. Four more washes of 10 min were done in MPBS, followed by DAPI staining that allows the visualization of the nucleus (10 min in 10 μg/mL of DAPI, followed by 10 min washing in MPBS). Staining was imaged in a Leica DM RxA2 confocal microscope (Wetzlar, Germany).

In Situ Hybridization

In situ hybridizations for *enod40* were performed as previously described (Crespi et al., 1994). The images were obtained by superposition of tissue autofluorescence (in red) and the epireflectance of silver grains (polarization analyzer, in yellow).

Biolistics, Confocal Microscopy, and Image Processing

Biolistic introduction of plasmid DNA into plant cells was done using the PDS-1000/He System (Bio-Rad). For each experiment, bombardments were done at least five times, and an average of 200 transformed cells were obtained per bombardment. Cells were observed 24 h later with a Leica DM RxA2 confocal microscope. Equimolar quantities of plasmids were used in all cases except for the pair MS2coat-GFP/MS2-RNA, where a 1:3 ratio was used to decrease background because of nonbound GFP. Leica confocal software was used for image acquisition and quantification of fluorescence profiles. Sequential scans were done when necessary. Spectral profiles were calculated in five cells, and at least 10 regions were analyzed for each cell. Data processing was done with Adobe Photoshop (Mountain View, CA) and Microsoft Excel.

The MtRBP1 sequence has been submitted to the EMBL Nucleotide Sequence Database under accession number AJ508392.

Sequence data from this article have been deposited with the EMBL/GenBank data libraries under accession number AJ508392.

ACKNOWLEDGMENTS

We thank J. Gyorgyey for the kind gift of the *M. truncatula* cDNA library, J. Podkowinski and A. Complainville for their contribution to preliminary three-hybrid screens, and M. Wickens, H. Spaink, and J. Hasselhoff for kindly providing various plasmids. We also thank C. Breda for her contribution to immunolocalization experiments, A. Expert for his advice in RNA pull down experiments, P. Mergaert for the cDNA from different nodule developmental stages, and S. Brown and C. Talbot of the Cellular Biology Platform (Institut Fédératif de Recherche) for their help in confocal microscopy. We also thank Florian Frugier and Claude Thermes for critical reading of the manuscript. A.C. was supported by a Marie Curie Individual Fellowship.

REFERENCES

Arn, E.A., and Macdonald, P.M. (1998). Motors driving mRNA localization: New insights from *in vivo* imaging. Cell **95,** 151–154.

Asad, S., Fang, Y., Wycoff, K.L., and Hirsch, A.M. (1994). Isolation and characterization of cDNAs and genomic clones of *MsENOD40*: Transcripts are detected in meristematic cells of alfalfa. Protoplasma **183,** 10–23.

Bertrand, E., Chartrand, P., Schaefer, M., Shenoy, S.M., Singer, R.H., and Long, R.M. (1998). Localization of ASH1 mRNA particles in living yeast. Mol. Cell **2,** 437–445.

Boisson-Dernier, A., Chabaud, M., Garcia, F., Becard, G., Rosenberg, C., and Barker, D.G. (2001). *Agrobacterium rhizogenes*-transformed roots of *Medicago truncatula* for the study of nitrogen-fixing and endomycorrhizal symbiotic associations. Mol. Plant Microbe Interact. **14,** 695–700.

Burd, C.G., and Dreyfuss, G. (1994). Conserved structures and diversity of functions of RNA-binding proteins. Science **265,** 615–621.

Cáceres, J.F., Screaton, G.R., and Krainer, A.R. (1998). A specific subset of SR proteins shuttles continuously between the nucleus and the cytoplasm. Genes Dev. **12,** 55–66.

Casson, S.A., Chillen, P.M., Topping, J.F., Evans, M., Souter, M.A., and Lindsey, K. (2002). The POLARIS gene of Arabidopsis encodes a predicted peptide required for correct root growth and leaf vascular patterning. Plant Cell **14,** 1705–1721.

Charon, C., Sousa, C., Crespi, M., and Kondorosi, A. (1999). Alteration of *enod40* expression modifies *Medicago truncatula* root nodule development induced by *Sinorhizobium meliloti*. Plant Cell **11,** 1953–1966.

Chinchilla, D., Merchan, F., Megias, M., Kondorosi, A., Sousa, C., and Crespi, M. (2003). Ankyrin protein kinases: A novel type of plant kinase gene whose expression is induced by osmotic stress in alfalfa. Plant Mol. Biol. **51,** 555–566.

Compaan, B., Yang, W.-C., Bisseling, T., and Franssen, H. (2001). *ENOD40* expression in the pericycle precedes cortical cell division in *Rhizobium*-legume interaction and the highly conserved internal region of the gene does not encode a peptide. Plant Soil **230,** 1–8.

Crespi, M., and Galvez, S. (2000). Molecular mechanisms in root nodule development. J. Plant Growth Regul. **19,** 155–166.

Crespi, M., Jurkevitch, E., Poiret, M., d'Aubenton-Carafa, Y., Petrovics, G., Kondorosi, E., and Kondorosi, A. (1994). *enod40*, a gene expressed during nodule organogenesis, codes for a non-translatable RNA involved in plant growth. EMBO J. **13,** 5099–5112.

Dirks, R.W., Molenaar, C., and Tanke, H.J. (2001). Methods for visualizing RNA processing and transport pathways in living cells. Histochem. Cell Biol. **115,** 3–11.

Dreyfuss, G., Kim, V.N., and Kataoka, N. (2002). Messenger-RNA-binding proteins and the messages they carry. Nat. Rev. Mol. Cell Biol. **3,** 195–205.

Eddy, S.R. (2002). Computational genomics of noncoding RNA genes. Cell **109,** 137–140.

Erdmann, V.A., Barciszewska, M.Z., Szymanski, M., Hochberg, A., de Groot, N., and Barciszewski, J. (2001). The non-coding RNAs as riboregulators. Nucleic Acids Res. **29,** 189–193.

Furini, A., Koncz, C., Salamini, F., and Bartels, D. (1997). High level transcription of a member of a repeated gene family confers dehydration tolerance to callus tissue of Craterostigma plantagineum. EMBO J. **16,** 3599–3608.

Gama-Carvalho, M., and Carmo-Fonseca, M. (2001). The rules and roles of nucleocytoplasmic shuttling proteins. FEBS Lett. **498,** 157–163.

Girard, G., Roussis, A., Gultyaev, A.P., Pleij, C.W., and Spaink, H.P. (2003). Structural motifs in the RNA encoded by the early nodulation gene *enod40* of soybean. Nucleic Acids Res. **31,** 5003–5015.

Gyorgyey, J., Vaubert, D., Jimenez-Zurdo, J.I., Charon, C., Troussard, L., Kondorosi, A., and Kondorosi, E. (2000). Analysis of *Medicago truncatula* nodule expressed sequence tags. Mol. Plant Microbe Interact. **13,** 62–71.

Hannon, G.J. (2002). RNA interference. Nature **418,** 244–251.

Haseloff, J., and Amos, B. (1995). GFP in plants. Trends Genet. **11,** 328–329.

Hirotsune, S., Yoshida, N., Chen, A., Garret, L., Sugiyama, F., Takahashi, S., Yagami, K., Wynshaw-Boris, A., and Yoshiki, A. (2003). An expressed pseudogene regulates the messenger-RNA stability of its homologous coding gene. Nature **423,** 91–96.

Joyce, G.F. (2002). The antiquity of RNA-based evolution. Nature **418,** 214–221.

Kelley, R.L., and Kuroda, M.I. (2000). Non-coding RNA genes in dosage compensation and imprinting. Cell **103,** 9–12.

Kiss, T. (2002). Small nucleolar RNAs: An abundant group of noncoding RNAs with diverse cellular functions. Cell **109,** 145–148.

Kouchi, H., Takane, K., So, R.B., Ladha, J.K., and Reddy, P.M. (1999). Rice *ENOD40*: Isolation and expression analysis in rice and transgenic soybean root nodules. Plant J. **18,** 121–129.

Leibovitch, M.P., Nguyen, V.C., Gross, M.S., Solhonne, B., Leibovitch, S.A., and Bernheim, A. (1991). The human ASM (adult skeletal muscle) gene: Expression and chromosomal assignment to 11p15. Biochem. Biophys. Res. Commun. **180,** 1241–1250.

Leighton, P.A., Ingram, R.S., Eggenschwiler, J., Efstratiadis, A., and Tilghman, S.M. (1995). Disruption of imprinting caused by deletion of the H19 gene region in mice. Nature **375,** 34–39.

Li, J., Kinoshita, T., Pandey, S., Ng, C.K., Gygi, S.P., Shimazaki, K., and Assmann, S.M. (2002). Modulation of an RNA-binding protein by abscisic-acid-activated protein kinase. Nature **418,** 793–797.

Lindsey, K., Casson, S., and Chilley, P. (2002). Peptides: New signaling molecules in plants. Trends Plant Sci. **7,** 78–83.

Lorkovic, Z.J., and Barta, A. (2002). Genome analysis: RNA recognition motif (RRM) and K homology (KH) domain RNA-binding proteins from the flowering plant Arabidopsis thaliana. Nucleic Acids Res. **30,** 623–635.

MacIntosh, G.C., Wilkerson, C., and Green, P.J. (2001). Identification and analysis of Arabidopsis expressed sequence tags characteristic of non-coding RNAs. Plant Physiol. **127,** 765–776.

Melcak, I., Melcakova, S., Kopsky, V., Vecerova, J., and Raska, I. (2001). Prespliceosomal assembly on microinjected precursor mRNA takes place in nuclear speckles. Mol. Biol. Cell **12,** 393–406.

Olivas, W.M., Muhlrad, D., and Parker, R. (1997). Analysis of the yeast genome: Identification of new non-coding and small ORF-containing RNAs. Nucleic Acids Res. **25,** 4619–4625.

Pederson, T. (2001). Fluorescent RNA cytochemistry: Tracking gene transcripts in living cells. Nucleic Acids Res. **29,** 1013–1016.

Rook, M.S., Lu, M., and Kosik, K.S. (2000). CaMKIIalpha 3′ untranslated region-directed mRNA translocation in living neurons: Visualization by GFP linkage. J. Neurosci. **20,** 6385–6393.

Rohrig, H., Schmidt, J., Miklashevichs, E., Schell, J., and John, M. (2002). Soybean *ENOD40* encodes two peptides that bind to sucrose synthase. Proc. Natl. Acad. Sci. USA **99,** 1915–1920.

Sanford, J.R., and Bruzik, J.P. (2001). Regulation of SR protein localization during development. Proc. Natl. Acad. Sci. USA **98,** 10184–10189.

Sato, M., Shinozaki-Yabana, S., Yamashita, A., Watanabe, Y., and Yamamoto, M. (2001). The fission yeast meiotic regulator Mei2p undergoes nucleocytoplasmic shuttling. FEBS Lett. **499,** 251–255.

Sengupta, D.J., Zhang, B., Kraemer, B., Pochart, P., Fields, S., and Wickens, M. (1996). A three-hybrid system to detect RNA-protein interactions *in vivo*. Proc. Natl. Acad. Sci. USA **93,** 8496–8501.

Shyu, A.B., and Wilkinson, M.F. (2000). The double lives of shuttling mRNA-binding proteins. Cell **102,** 135–138.

Sousa, C., Johansson, C., Charon, C., Manyani, H., Sautter, C., Kondorosi, A., and Crespi, M. (2001). Translational and structural requirements of the early nodulin gene *enod40*, a short-open reading frame-containing RNA, for elicitation of a cell-specific growth response in the alfalfa root cortex. Mol. Cell. Biol. **21,** 354–366.

Tenson, T., DeBlasio, A., and Mankin, A. (1996). A functional peptide encoded in the Escherichia coli 23S rRNA. Proc. Natl. Acad. Sci. USA **93,** 5641–5646.

van de Sande, K., Pawlowski, K., Czaja, I., Wieneke, U., Schell, J., Schmidt, J., Walden, R., Matvienko, M., Wellink, J., van Kammen, A., Franssen, H., and Bisseling, T. (1996). Modification of phytohormone response by a peptide encoded by *ENOD40* of legumes and a nonlegume. Science **273,** 370–373.

Watanabe, T., Miyashita, K., Saito, T.T., Yoneki, T., Kakihara, Y., Nabeshima, K., Kishi, Y.A., Shimoda, C., and Nojima, H. (2001). Comprehensive isolation of meiosis-specific genes identifies novel proteins and unusual non-coding transcripts in Schizosaccharomyces pombe. Nucleic Acids Res. **29,** 2327–2337.

Yamashita, A., Watanabe, Y., Nukina, N., and Yamamoto, M. (1998). RNA-assisted nuclear transport of the meiotic regulator Mei2p in fission yeast. Cell **95,** 115–123.

Zalfa, F., Giorgi, M., Primerano, B., Moro, A., Di Penta, A., Reis, S., Oostra, B., and Bagni, C. (2003). The fragile X syndrome protein FMRP associates with BC1 RNA and regulates the translation of specific mRNAs at synapses. Cell **112,** 317–327.

Zeng, C., Kim, E., Warren, S.L., and Berget, S.M. (1997). Dynamic relocation of transcription and splicing factors dependent upon transcriptional activity. EMBO J. **16,** 1401–1412.